Environmental Influence on the Surface Chemistry of Ionic- Liquid-Mediated Lubrication in a Silica / Silicon Tribopair

ARTICLE *in* THE JOURNAL OF PHYSICAL CHEMISTRY C · JULY 2014

Impact Factor: 4.77

THE JOURNAL OF PHYSICAL CHEMISTRY C

Article

pubs.acs.org/JPCC

Environmental Influence on the Surface Chemistry of Ionic-Liquid-Mediated Lubrication in a Silica/Silicon Tribopair

Andrea Arcifa,[†] Antonella Rossi,[†,‡] Rosa M. Espinosa-Marzal,[†,§] and Nicholas D. Spencer*[,†]

[†]Lab. for Surface Science and Technology, Dept. of Materials, ETH Zurich, CH-8093 Zurich, Switzerland

[‡]Dipartimento di Scienze Chimiche e Geologiche, Università di Cagliari, 09042 Cagliari, Italy

[§]Laboratory for Smart Interfaces in Environmental Nanotechnology, Department of Civil & Environmental Engineering, University of Illinois at Urbana−Champaign, Champaign, Illinois 61801, United States

Supporting Information

ABSTRACT: In this study, 1-ethyl-3-methyl imidazolium trifluoro tris-(pentafluoroethyl) tris(perfluoroalkyl)trifluorophosphate [EMIM] FAP and 1-hexyl-3-methyl imidazolium tris(pentafluoroethyl) tris(perfluoroalkyl)-trifluorophosphate [HMIM] FAP were selected as lubricants for silica/silicon surfaces. Pin-on-disk tribometry was used to test the performance of these lubricants under two different environmental conditions (humid air and a nitrogen atmosphere). The surface reactivity of the ionic liquids under mechanical stress was investigated ex situ by X-ray photoelectron spectroscopy. Environmental conditions appear to affect the mechanism of boundary lubrication in different ways, depending on the contact pressure. Tests carried out at 0.5 N applied load showed low friction and no detectable wear in a nitrogen atmosphere, and a substantial increase in both wear and friction in humid air. It is proposed that the presence of water in the IL induces a change in the structure of the confined lubricant film, leading to contact between the sliding surfaces. At higher load (4.5 N), the observation of wear, both under nitrogen and in humid air, reveals that the film is no longer able to prevent contact between asperities, which now dominates the observed tribological behavior. XP-spectra acquired on samples tribostressed at high load, under the two environmental conditions, reveal evidence for the formation of a reaction layer that is hydrolyzed or oxidized in the presence of water and oxygen, suggesting that the variation of wear with the environment is related to changes in the tribochemical reactions involving the silicon surface.

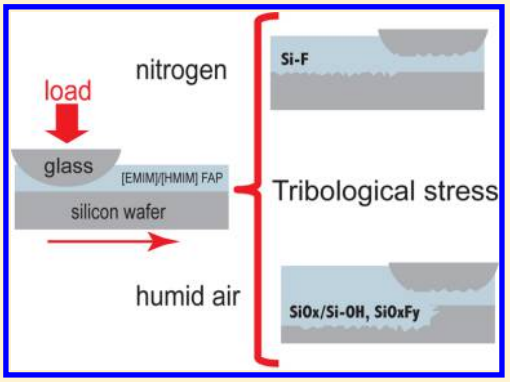

1. INTRODUCTION

Room-temperature ionic liquids (ILs) are molten salts having melting points that lie at room temperature or below. As a result of the asymmetrical shape and large dimension of at least one of the ions, packing into a regular lattice is inhibited and the electrostatic interactions between ions are weakened, thus inhibiting crystallization.

The introduction of air-stable ILs,[1] and the subsequent availability of a large variety of structures and functionalities,[2] triggered the interest of many researchers in understanding the physical properties of ILs and testing them for several applications.[3,4] ILs generally exhibit high thermal stability, negligible vapor pressure, and nonflammability.[5] These properties are highly desirable in lubrication, especially for applications involving extreme conditions, such as high temperatures or low pressures. Consequently, the tribological performance of ILs has been extensively investigated over the past decade.[6,7]

In addition to the above-mentioned properties, for a liquid to be used as a lubricant, it must also be suited to function over the range of operating conditions encountered in the application of interest. As a first requirement, the lubricant must be chemically compatible with the materials involved. In this regard it should be noted that the presence of water and oxygen absorbed from air can lead to extensive corrosion of some materials over long exposure times—an issue that seems to be frequently neglected in the case of ionic-liquid lubrication.[8] Furthermore, the lubricant should be able to prevent wear and provide low friction, even when the surfaces come into physical contact, that is, in the boundary-lubrication regime. Depending on the operating conditions, good tribological performance can be achieved either by the formation of a boundary layer that is able to effectively prevent direct contact between asperities, or by the formation of a tribolayer as a consequence of reactions taking place between the sliding surfaces and constituents of the lubricant (including, if present, additives and impurities).

Several studies have shown that many ILs exhibit a layered structure under nanoconfinement:[9−11] the ion tends to remain between the surfaces, preventing direct contact between

Special Issue: John C. Hemminger Festschrift

Received: June 17, 2014
Revised: July 30, 2014
Published: July 30, 2014

asperities. In our laboratory, by using the surface forces apparatus technique, it has been recently demonstrated for several ILs that dissolved water influences the structure of the nanoconfined IL film and the dynamics of the film-thickness transitions,[12,13] suggesting that the ability of the confined liquid to separate the two hydrophilic surfaces can be affected by the presence of water, even in the case of hydrophobic ILs. It is worthwhile mentioning that the pressure range in those nanotribological experiments (atomic force microscopy and surface forces apparatus) lies at least 1 order of magnitude below that in the tribological studies described in this work, and also that mica surfaces were employed.

Evidence of layering and changes in the dynamic properties of IL confined between silica surfaces have also been reported by using surface-forces and shear-resonance measurements[14] for two hydrophobic ILs, although in this case the experiments were carried out under ambient conditions and the effect of water content was not discussed.

Under harsher, boundary-lubrication conditions, the chemical processes taking place within the contact area can determine the tribological behavior. Understanding these tribochemical reactions is of paramount importance, as they can be either detrimental or useful for lubrication. Even under such conditions, the environment can play a decisive role, as the reaction mechanism can be affected by the presence of reactive species, such as oxygen and water.

An interesting result has been published by Kondo et al.[15] in the case of the lubrication of bearing steel by fluorinated ILs. Lubricity of these ILs was found to be superior to that observed for several halogen-free ILs. Iron fluoride was detected on samples tribostressed either in nitrogen or humid air, but higher wear was measured in the latter case. Additionally, tribostressed samples left in contact with humid air were affected by severe corrosion, indicating that the iron fluoride, despite its beneficial effect in terms of wear prevention during the tests, hydrolyzes when exposed to a humid environment, promoting the corrosion of the entire surface that had been in contact with the lubricant.

A significant number of investigations has been devoted to the study of ILs as lubricants for silicon-based materials.[6,16] These studies are motivated by the search for an effective lubricant for microelectromechanical systems (MEMS), which are generally fabricated from silicon by well-developed lithographic and micromachining techniques.[17] In the absence of lubricants, water is known to significantly enhance the wear of bare silicon oxide surfaces.[18] Nonetheless, the role of environmental conditions in the tribological behavior of silicon oxide surfaces lubricated with ILs has not been thoroughly investigated to date.

In the present work, the results obtained for two imidazolium-based ILs that differ in the aliphatic chain length attached to the imidazolium unit have been investigated. The effect of environmental conditions on the tribological behavior of silicon/silica tribopairs has been explored by comparing the results obtained in the presence of nitrogen and humid air. The influence of applied contact pressure has been taken into consideration by comparing results obtained under different loads. Friction and wear data are presented and discussed, together with the surface-chemical analysis of tribologically stressed samples at high load.

2. EXPERIMENTAL SECTION

2.1. Materials. 1-ethyl-3-methyl imidazolium trifluoro tris(perfluoroalkyl)trifluorophosphate ([EMIM] FAP) and 1-hexyl-3-methyl imidazolium tris(pentafluoroethyl) tris-(perfluoroalkyl)trifluorophosphate ([HMIM] FAP) were selected as lubricants. These classes of compounds are known to be among the most hydrophobic ILs available. Nonetheless, when exposed to humid air, the liquids absorb a measurable amount of water, as reported in Table 1.

Table 1. Viscosity and Density of Dry ILs and Measured Water Content Following 7 Days Equilibration at 45% RH Prior to Tribological Tests

selected ILs (supplier)	viscosity[a] (mPa·s)	density[b] g/cm^3	water content (%w/w)
[EMIM] FAP (Merck, Darmstadt, Germany)	75	1.720	0.07
[HMIM] FAP (Merck, Darmstadt, Germany)	116	1.560	0.08

[a]Viscosity data at 25 °C for dried ILs, data from the supplier. [b]Density data for dried ILs at 25 °C, data from the supplier.

As-received ILs were dehydrated by placing about 1 cm^3 of each IL into a sealed vessel connected to a rotary pump ($\sim 10^{-2}$ mbar). Drying was carried out for 3 days at a temperature of 45−50 °C, after an initial pre-evacuation at room temperature for about 5 h. The sealed vessel was then transferred to a nitrogen-filled glovebox (water and oxygen content lower than 10 ppm), where the vials were sealed and stored. Water content of the ILs, as measured by Karl Fischer titration, was found to be below 100 ppm. IL samples (about 0.4 cm^3) used for tribological experiments carried out in the presence of humid air were stored at a relative humidity of 45% (23 ± 2 °C) inside a sealed vessel containing a saturated solution of potassium carbonate. The water content after an exposure of 1 week is reported in Table 1.

For the tribological experiments, p-type (100)-oriented silicon wafers (Silicon Materials, Kaufering, Germany; root-mean-square roughness, R_q below 1 nm; size 15 × 10 mm^2) and fused-silica-glass spheres of 2 mm diameter (Corning 7980, J. Hauser GmbH & Co. Solms, Germany; $R_q \sim 1.1$ nm, as measured by atomic force microscopy) were used as disks and pins, respectively. The relevant mechanical and morphological properties are reported in Table 2.

Before the tribological experiment, the silicon wafers were sonicated for 5 min each in toluene and isopropanol, while the fused-silica-glass spheres were rinsed with isopropanol. The two surfaces were O_2-plasma treated for 2 min shortly before the test.

Table 2. Mechanical and Morphological Parameters of the Tribological Pairs Investigated

	material	R_q (nm)	Young's modulus (GPa)	Poisson's ratio	Knoop hardness (100 g) kg/mm^2
disk	silicon (100)	<1	130[a]	0.280[a]	964[b]
pin	fused silica	1.1 ± 1	72[b]	0.160[b]	533[c]

[a]Data from Hopcrof et al.[19] [b]Data from the supplier. [c]Data from Giardini et al.[20]

dx.doi.org/10.1021/jp505998k | J. Phys. Chem. C 2014, 118, 29389−29400

2.2. Methods. *2.2.1. Tribological Experiments.* Tribological experiments were performed using an UMT-2 Tribometer (Bruker Nano Inc., formerly Center of Tribology Inc., Campbell, U.S.A.) operating in pin-on-disk mode. Tests were carried out at two different applied loads (0.5 and 4.5 N, corresponding to a maximum Hertzian contact pressure of 640 and 1330 MPa, respectively), at a constant speed of 50 mm/min and a duration of 200 rotational cycles (radius of the track: 3.2 mm).

A load cell with a maximum capacity of 5 N and resolution of 0.0049 N (data from the manufacturer) was used. The calibration of the load cell was carried out using standard weights. Before each test, the misalignment of the disk with respect to the plane normal to the pin axis was checked by pressing down a steel stylus over two rotational cycles and evaluating the displacement of the z-axis required to maintain the load at a constant value (applied load, 200 mN; speed, 30; radius, 4.4 mm). In the case of a normal displacement larger than ± 10 μm, the planarity was adjusted by placing metal foils of known thicknesses between the sample holder and rotational drive. Before each tribological test, a volume of ~ 20 mm^3 of lubricant was placed on the disk such that the liquid was covering the entire surface.

The same instrumental parameters were adopted for two different environmental conditions: nitrogen atmosphere (water and oxygen content below 10 ppm) and humid air (45−55% RH; $T = 296 \pm 2$ K). The nitrogen atmosphere was achieved by placing the tribometer inside a MBraun Labmaster 100 glovebox filled with nitrogen.

Tribologically stressed samples tested in humid air were rinsed with ethanol and dried with nitrogen; those tested in the glovebox were rinsed with ethanol and vacuum-dried in order to avoid exposure to air. All tribological tests reported in this work were repeated at least three times. In the present work, friction trends with time are reported according to the following data-reduction method: the average value of the coefficient of friction (CoF) in each cycle was calculated, together with the associated standard deviation. Per-cycle-averaged CoF values are presented versus number of cycles during the tribological test.

2.2.2. Wear Analysis: Profilometry, Optical Microscopy, and Scanning Electron Microscopy (SEM). A Sensofar PLu Neox (Sensofar-Tech, SL, Terrassa, Spain) 3D optical profiler was used for characterizing the surface of the tribologically stressed samples at the end of the tests. Data were acquired by using SensoSCAN software (v.3.1.1.1, Sensofar-Tech, SL, Terrassa, Spain) and processed by SensoMAP software (v.5.1.1. Digital Surf, Besancon, France). 3D images of worn disks were collected in phase-shifting interferometry (PSI) mode, using a 10× objective.

An AX10 Imager M1m (Carl Zeiss, Oberkochen, Germany) with objectives ranging from 5× to 40× and equipped with a CCD camera was used for acquiring optical images.

Scanning electron microscopy (SEM) measurements were carried out with a Zeiss Gemini 1530 FEG SEM (5 kV acceleration voltage). An in-lens detector was used for the acquisition of the micrographs. Worn samples were coated with 3 nm of platinum prior to SEM analysis.

2.2.3. X-ray Photoelectron Spectroscopy. X-ray photoelectron spectroscopy was used for investigating the surface chemistry of contact and noncontact areas of tribologically stressed disks.

The X-ray photoelectron spectra presented in this work were acquired with a PHI Quantera SXM (ULVAC-PHI, Chanhassen, MN, U.S.A.). Analyses were carried out with a monochromatic Al Kα (1486.6 eV) source, using a beam diameter of 20 μm, the analyzer working in constant-analyzer-energy (CAE) mode. The pass energy and the step size were 69 and 0.125 eV, respectively (full-width-at-half-maximum (fwhm) of the peak height for Ag $3d_{5/2}$ = 0.71 eV). Survey spectra were acquired with a pass energy of 280 eV and a step size of 1 eV. In both cases, the emission angle was 45°. The spectrometer was calibrated according to ISO 15472:2001 with an accuracy of ± 0.1 eV.

X-ray-induced secondary electron imaging (SXI) was used to locate the desired analysis region, taking advantage of the possibility to locate small features within the wear track.

As the contact area was found to be affected by differential charging, the disks were mounted on the sample holder by using double-sided adhesive tape and the analyses were carried out while using a low-voltage argon ion gun/electron neutralizer. The results here presented were collected in debris-free scar areas.

The energy scales of all the spectra are referred to elemental Si $2p_{3/2}$ (99.3 eV), as found for tests carried out in the absence of charge compensation and in agreement with the literature.[21] Carbon was not selected for referencing, as the chemical nature of the carbon-containing species, especially with regard to the tribostressed areas, was unknown a priori. Nonetheless, when considering the position of the maximum of the most intense C 1s component, either in the contact or in the noncontact area, shifts of less than ± 0.2 eV from the value expected for aliphatic carbon were observed.

The high-resolution spectra were processed using CasaXPS software (v.2.3.15, Casa Software Ltd., Wilmslow, Cheshire, U.K.). The line shapes used for the curve fitting are reported in Tables S1 and S2 (Supporting Information).

3. RESULTS

3.1. Tribological Testing. *3.1.1. Tribotest at 0.5 N: Friction and Wear Analysis. Nitrogen Atmosphere.* Nearly constant COF values of 0.10 (0.02) and 0.09 (0.01) for [EMIM] FAP and [HMIM] FAP, respectively, were observed for the entire duration of the tests carried out at a load of 0.5 N in a nitrogen atmosphere (Figure 1a,b, black curves), with only small per-cycle scatter of friction data (represented by the error bars associated with each point of the curves in Figure 1a,b). The CoF appears to be not significantly affected by the length of the alkyl chain attached to the imidazolium unit. At the end of the test (200 cycles), wear of the disk was found to be undetectable in optical micrographs, and therefore no attempt was made to quantify the wear coefficient.

Humid-Air Tests. For both tested ILs, the CoF was found to increase initially, reaching an approximately constant value during the final part of the test. Taking the average value over the last 50 turns, [EMIM] FAP and [HMIM] FAP exhibited mean COF values of 0.23 (0.01) and 0.27 (0.01), respectively.

With regard to the initial part of the test, while a relatively rapid increase of friction was always observed in the case of [EMIM] FAP, in the presence of [HMIM] FAP, an initial regime of low friction was measured, whose value was close to that obtained under dry conditions. The duration of this initial phase varied significantly for repeated tests (Figure S1, Supporting Information). Wear tracks formed on the silicon wafers during tests carried out in humid air were clearly

dx.doi.org/10.1021/jp505998k | J. Phys. Chem. C 2014, 118, 29389−29400

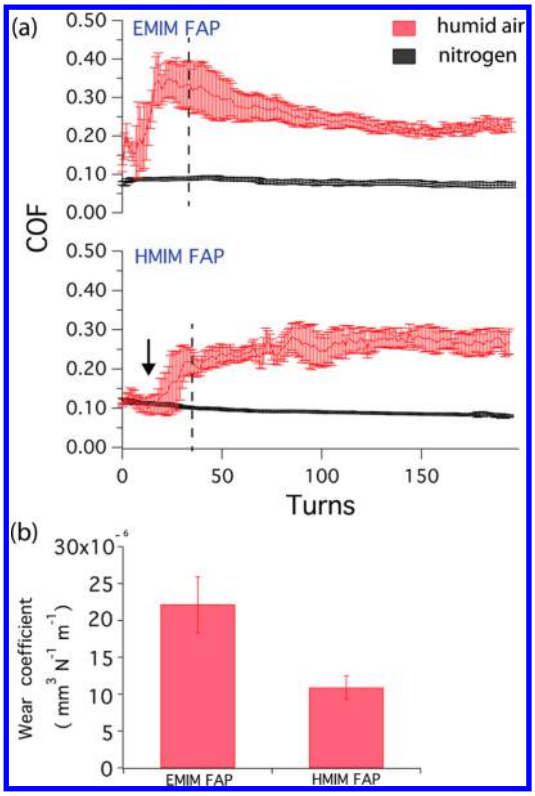

Figure 1. (a) Coefficient of friction vs number of sliding cycles during tribological tests (normal load, 0.5 N; sliding speed, 50 mm/min; duration, 200 turns; radius, 3.2 mm) carried out in the presence of [EMIM] FAP and [HMIM] FAP (b) at room temperature (296 ± 2 K) and two different environmental conditions: humid air (45−55% RH, red curve) and nitrogen atmosphere (black curve). Error bars express the standard deviation of friction data over one cycle. Vertical lines indicate the transitions observed in the presence of humid air from an initial regime characterized by an increase of friction upon time to a steady-state condition. The arrow indicates the initial low-friction regime observed for HMIM FAP (c) wear coefficient of the disk measured after tribological tests carried out in the presence of humid air, as measured by optical profilometry.

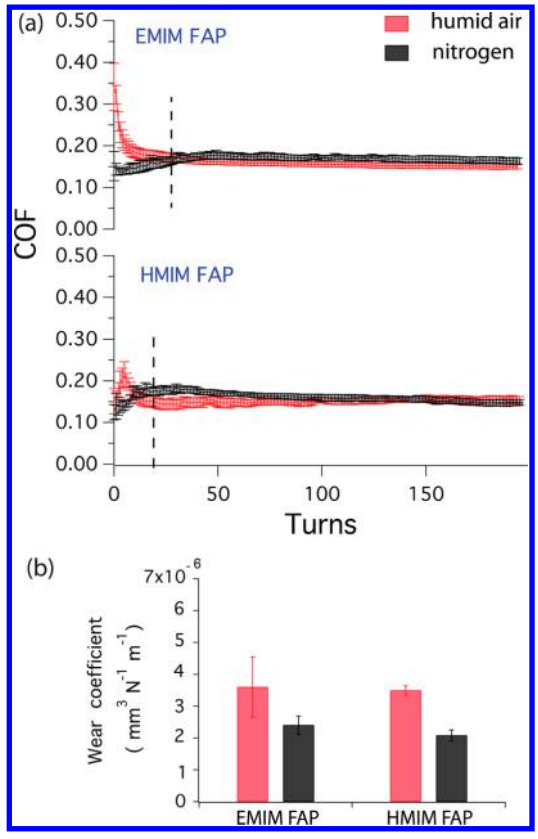

Figure 2. (a) Coefficient of friction vs number of sliding cycles during tribological tests (normal load, 4.5 N; sliding speed, 50 mm/min; duration, 200 turns; radius, 3.2 mm) carried out in the presence of [EMIM] FAP and [HMIM] FAP (b) at room temperature (296 ± 2 K) and two different environmental conditions: humid air (45−55% RH, red curve) and nitrogen atmosphere (black curve). Vertical lines indicate the transitions from an initial regime characterized by a variation of friction upon time to a steady-state condition. Error bars express the standard deviation of friction data over one cycle. (b) Wear coefficient of the disk measured after tribological tests carried out in the presence [EMIM] FAP and [HMIM] FAP according to the conditions reported above, as measured by optical profilometry.

detectable by profilometry. Wear coefficients of 2.2 (0.4) × 10^{-5} and 1.1 (0.2) × 10^{-5} mm^3 m^{-1} N^{-1} were measured for disks lubricated with [EMIM] FAP and [HMIM] FAP, respectively (Figure 1c).

The wear coefficients of the fused silica pins were found to be similar in the two cases: 5 (2) and 3.8 (0.7) × 10^{-7} mm^3 m^{-1} N^{-1} for [EMIM] FAP and [EMIM] FAP, respectively.

3.1.2. Tribotest at 4.5 N: Friction and Wear Analysis. Figure 2a,b display the evolution of the CoF during tribological experiments performed at a load of 4.5 N, together with the corresponding wear coefficient of the silicon disk, measured after the test by optical profilometry.

For both ILs and under both environmental conditions, the CoF trends exhibited an initial phase of around 20−50 turns during which friction was found to change over time. Interestingly, these initial trends were found to be closely related to the environmental conditions and the kind of lubricant (see Figures S2−5, Supporting Information).

After the initial turns, a steady-state phase was observed for all tests, with relatively small per-cycle scatter of friction data: the differences in the measured CoF values in the presence of nitrogen atmosphere and humid air respectively were found to be small, considering the experimental variability of the data. In the presence of humid air, taking the average value over the last 50 turns, [EMIM] FAP and [HMIM] FAP exhibited mean COF values of 0.15 (0.01) and 0.16 (0.02), respectively. For tests carried out in the presence of a nitrogen atmosphere, the two ILs exhibited mean COF values of 0.165 (0.03) and 0.149 (0.03).

When switching from nitrogen to humid air, an increase of wear rate of the disks was measured in both cases (Figure 2c). In humid air, wear coefficients of the silicon disks were found to be 3.6 (0.9) × 10^{-6} and 3.5 (0.1) × 10^{-6} mm^3 m^{-1} N^{-1} for [EMIM] FAP and [HMIM] FAP respectively, while in the presence of a nitrogen atmosphere 2.4 (0.3) × 10^{-6} and 2.1 (0.1) × 10^{-6} mm^3 m^{-1} N^{-1} were measured.

Wear of the silica glass pins was found to be not significantly affected by the change in environmental conditions. In humid air, wear coefficients of the pins were found to be 9 (2) × 10^{-7} and 6 (2) × 10^{-7} mm^3 m^{-1} N^{-1} for [EMIM] FAP and [HMIM] FAP, respectively, while in the presence of a nitrogen atmosphere a value of 6 (1) × 10^{-7} mm^3 m^{-1} N^{-1} was found in both cases.

3.2. Morphology of the Worn Areas: Optical and Electron Microscopy. Figures 3 and 4 show the appearance

dx.doi.org/10.1021/jp505998k | J. Phys. Chem. C 2014, 118, 29389−29400

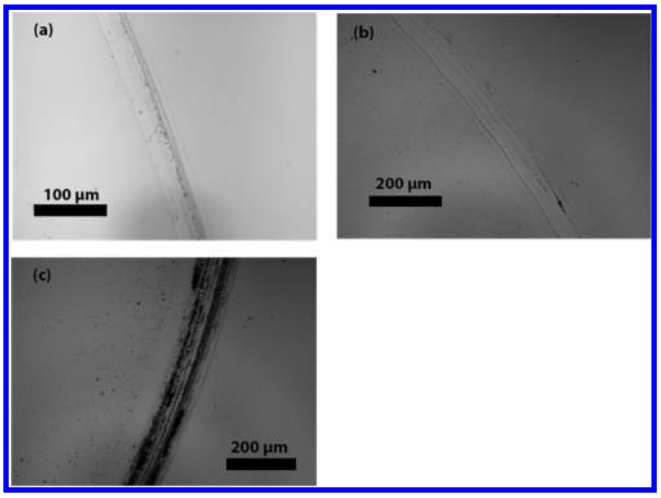

Figure 3. Optical micrographs of the contact area of silicon wafers lubricated with [HMIM] FAP: (a) normal load, 0.5 N; environment, humid air (45−55% RH); (b) normal load, 4.5 N; environment, nitrogen atmosphere; (c) normal load, 4.5 N; environment, humid air (45−55% RH). All the tests were performed at a sliding speed of 50 mm/min and a duration of 200 cycles (radius: 3.2 mm).

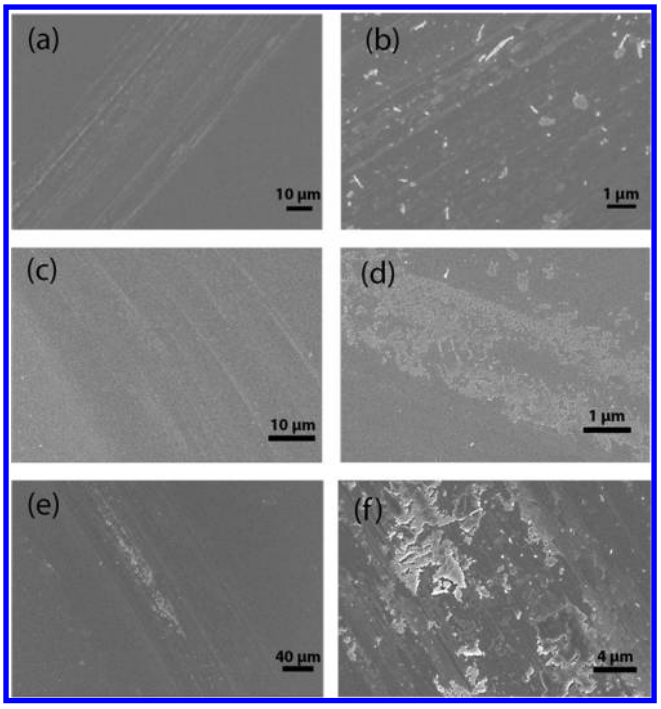

Figure 4. SEM images of the contact area of silicon wafers lubricated with [HMIM] FAP: (a, b) normal load, 0.5 N; environment, humid air (45−55% RH); (c, d) normal load, 4.5 N; environment, nitrogen atmosphere; (e, f) normal load, 4.5 N; environment, humid air (45−55% RH). All the tests were performed at a sliding speed of 50 mm/min and for a duration of 200 cycles (radius: 3.2 mm).

of the wear track as detected by optical and scanning electron microscopy, respectively. The results found for the two ILs are qualitatively very similar and only the pictures of the samples lubricated with [HMIM] FAP are discussed in the following (micrographs of the samples lubricated with [EMIM] FAP are provided in the Supporting Information, Figures S9 and S10). Additionally, as mentioned above, no detectable wear was observed on the surface of disks tribostressed under nitrogen when applying a load of 0.5 N and no images related to this set of tests are reported here.

Wear tracks produced on samples tribostressed in the presence of humid air exhibited a large number of parallel grooves within the track (Figures 3 and 5), while the tracks

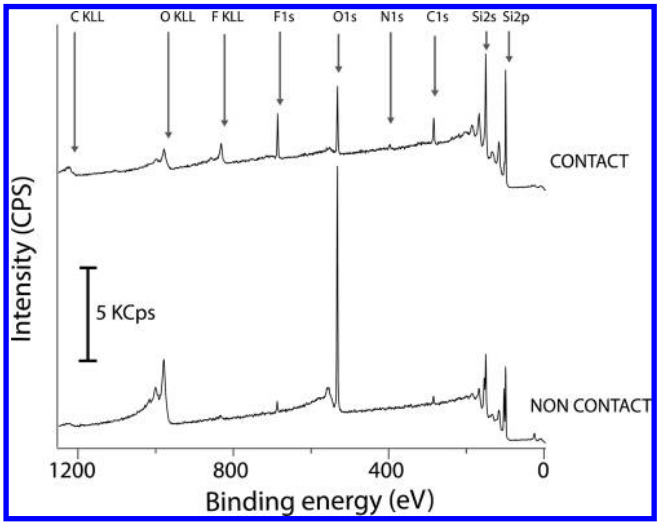

Figure 5. Survey XP-spectra of a silicon disk lubricated with [HMIM] FAP under a nitrogen atmosphere: normal load, 4.5 N; sliding speed, 50 mm/min; number of cycles, 200; radius, 3.2 mm.

obtained under nitrogen were smoother (Figure 4). Comparing the scars formed under different environmental conditions when applying a load of 4.5 N, a larger amount of debris was found within the contact area in the case of tests performed in the presence of humid air.

3.3. X-ray Photoelectron Spectroscopy (XPS). *3.3.1. X-ray Photoelectron Spectroscopy of Tribostressed Silicon Wafers.* Figure 5 illustrates the survey spectra acquired in the contact and noncontact areas of a silicon wafer tribostressed with a fused-silica-glass pin in the presence of [HMIM] FAP as a lubricant and under a nitrogen atmosphere. The load was maintained constant at 4.5 N during the test (200 turns, with radius of 3.2 mm).

Both spectra showed the presence of peaks characteristic of silicon oxide and silicon, (Si 2p, Si 2s and O 1s). The intensity of the O 1s signal is lower in the case of the tribostressed area, indicating the removal of the oxide layer from the substrate during sliding. The thickness of the layer was calculated to be of 1.5 (0.2) nm from the intensity ratio of silica to silicon signal, corrected for the density of the materials and for the inelastic mean free path in the noncontact area.

Additionally, while fluorine signals were observed in both spectra, the characteristic nitrogen peak (N 1s) was clearly detected only in the spectra of the contact area. The high-resolution spectra for the same sample are reported in Figure 6 and 7.

The C 1s signal in the noncontact area (Figure 6a) consisted of a superposition of several components originating from aliphatic carbon (285.0 (0.2) eV) and carbon bonded to oxygen or nitrogen.[22] The binding energies of these two components were constrained at a distance of +1.3 and +2.6 eV from the aliphatic signal, respectively, while their width was maintained at the same value (1.4 eV).

When considering the contact area, an additional component at the lower-binding-energy side was required in order to fit the

dx.doi.org/10.1021/jp505998k | J. Phys. Chem. C 2014, 118, 29389−29400

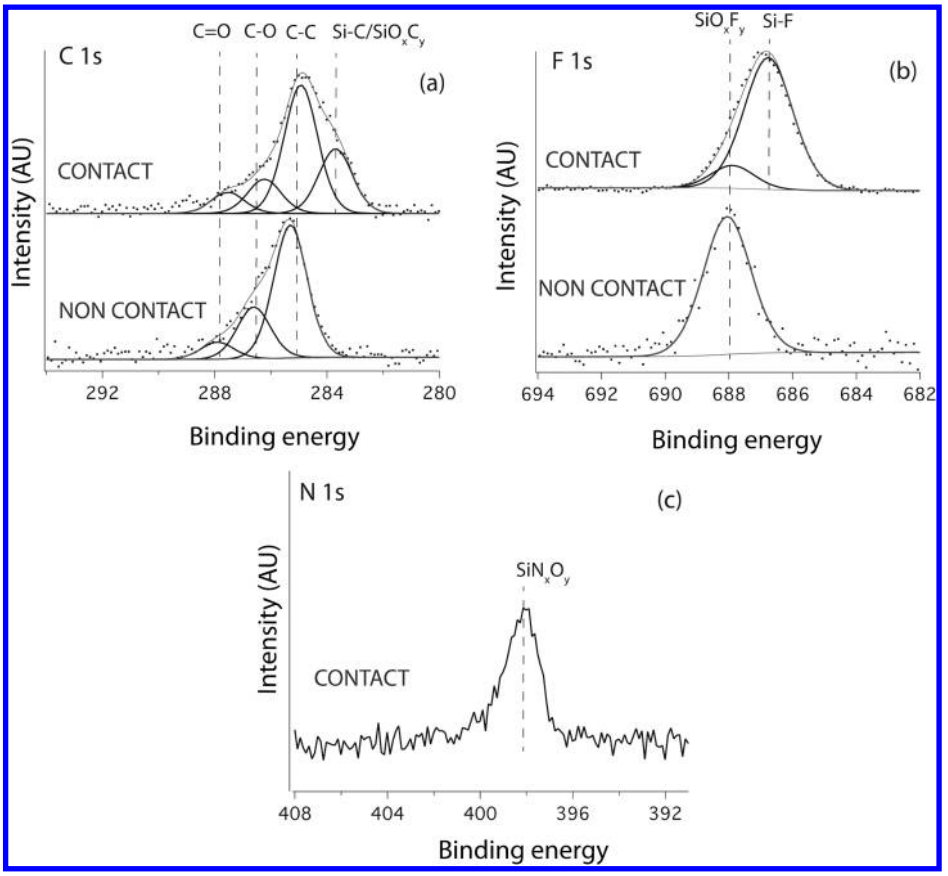

Figure 6. C 1s (a), F 1s (b), and N 1s (c) regions of the XP-spectra of a silicon disk lubricated with [HMIM] FAP under a nitrogen atmosphere. The nitrogen N 1s signal was not detected in the noncontact area. Normal load, 4.5 N; sliding speed, 50 mm/min; number of cycles, 200; radius, 3.2 mm.

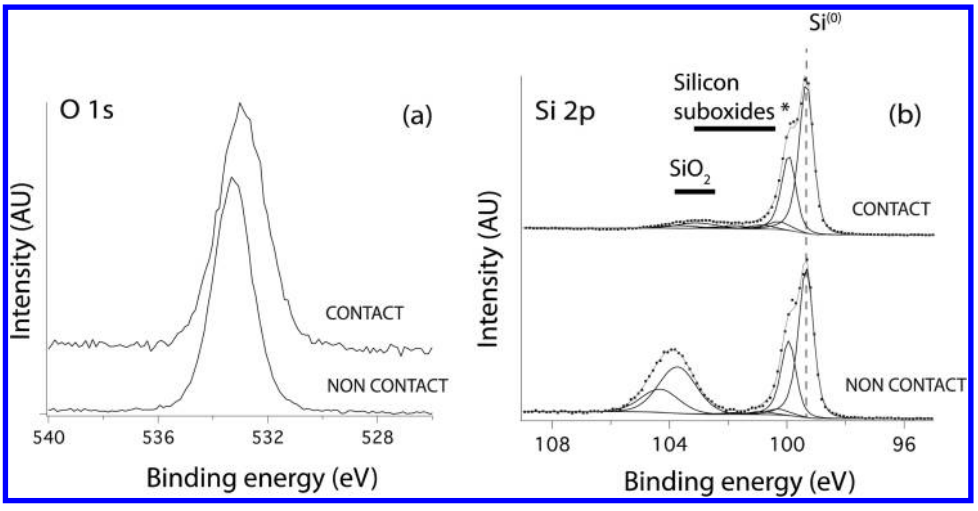

Figure 7. O 1s (a) and Si 2p (b) XP-spectra of a silicon disk lubricated with [HMIM] FAP under a nitrogen atmosphere. Each Si signal is fitted with two components due to spin−orbit coupling ($2p_{3/2}$ and $2p_{1/2}$). The region labeled as "Silicon suboxides" could also contain contributions from SiO_xF_y, SiC_xO_y, SiN_xO_y. Normal load, 4.5 N; sliding speed, 50 mm/min; normal load, 4.5 N; sliding speed, 50 mm/min; number of of cycles, 200; radius, 3.2 mm.

spectra, which revealed the formation of a new compound with peak position 283.8 eV.

The F 1s signal of the noncontact area consisted of a single peak centered at 687.9 (0.1) eV. Both the shape of the signal and its position on the binding-energy scale are different from those observed for the pure IL (not shown), indicating the presence of a different chemical species.

The F 1s spectra acquired in the contact area are broader and shifted toward lower binding-energy values than those of the noncontact area. Adopting the same model used for fitting the spectra of the noncontact area, an additional peak centered at 686.8 (0.1) eV is needed to fit the signal (Figure 6b).

The N 1s signal (Figure 6c) was clearly observed only in the spectra taken from the contact area. It consists of a peak with a maximum at 398.2 (0.1) eV. This peak cannot be related to the

dx.doi.org/10.1021/jp505998k | J. Phys. Chem. C 2014, 118, 29389−29400

presence of imidazolium cations, as a large shift is observed when comparing its position on the binding-energy scale with that of pure [HMIM] FAP (not shown, binding energy: 402.2 (0.1) eV).

The oxygen 1s signal (Figure 7a) of the noncontact area (binding energy = 533.1 (0.1) eV) mainly coincided with that measured for bare O_2 plasma-treated silicon samples: no relevant line-shape changes due to the presence of fluorine-containing adsorbed species could be detected. The oxygen 1s spectra acquired inside the contact area exhibited a peak broader than that of the noncontact area and slightly shifted toward lower binding energy (binding energy = 532.9 (0.1) eV). The broadening might derive from the higher variability of the local chemical environment present inside the wear track. Additionally, the large range of thickness for the oxide layer is expected to result in a broadening toward lower binding energy, as the SiO_2 signals monotonically depend on the thickness of the oxide layer.[21,23]

The silicon 2p signal (Figure 7b) of the noncontact area is consistent with the presence of a silicon oxide layer covering the silicon substrate. The component associated with the silicon dioxide is centered at 103.6 (0.2) eV. The presence of silicon suboxides (Si^{+}, Si^{2+}, Si^{3+}), whose binding energies were fixed according to the procedure reported by Seah et al.[24] (binding energies: 100.3, 101.2, 101.8 eV, respectively) accounts for less than 4% of the overall intensity. It has to be noted that the selected background and line shape of the signals could differ from those actually present, resulting in a large uncertainty in the estimation of the small intensity of the suboxide signals.

When considering the contact area, the main observation concerns the drop in intensity of the Si^{4+} component compared to that of Si^{0} and its shift toward lower binding energy (103.2 (0.2) eV). Additionally, a slight increase in the intensity of the signal in the energy range between the Si 2p (Si^{0}) and Si 2p (Si^{4+}) was observed.

The chemical-state analysis of silicon, especially with regard to the part of the spectrum attributed to the silicon at intermediate oxidation states (Si^{1+}, Si^{2+}, Si^{3+}) is hindered by the fact that the 2p peaks associated with Si−F have chemical shifts similar to those of the suboxides (100.4, 101.5, and 102.6 eV for SiF, SiF_2, and SiF_3, respectively[25]), giving rise to an overlap of signals that could also include components related to Si−C, if present (100.2−101.4 eV, see Table S3, Supporting Information). In addition to this, the above-mentioned uncertainty concerning line shapes and background further complicates the interpretation of this spectral range. With regard to the curve-fitting model proposed in Figure 7b (contact area), the same components used for the dioxide and suboxides are assumed to represent the multitude of chemical environments expected for silicon in different chemical states. In this way, an increase in the contribution related to the intermediate oxidation state can be observed, but no precise assignments to specific species are proposed here. The component associated with Si^{4+} shifts toward lower binding energy. As in the case of the oxygen O 1s, the decrease in oxide thickness may account for this observation, but also a change in the chemical environment cannot be ruled out.

Some significant differences in the chemical composition of both contact and noncontact areas were observed when considering the surface characterization of silicon disks tribostressed in the presence of humid air using the same load and speed conditions. Figure 8 illustrates the survey spectra acquired in both contact and noncontact areas for this kind of sample.

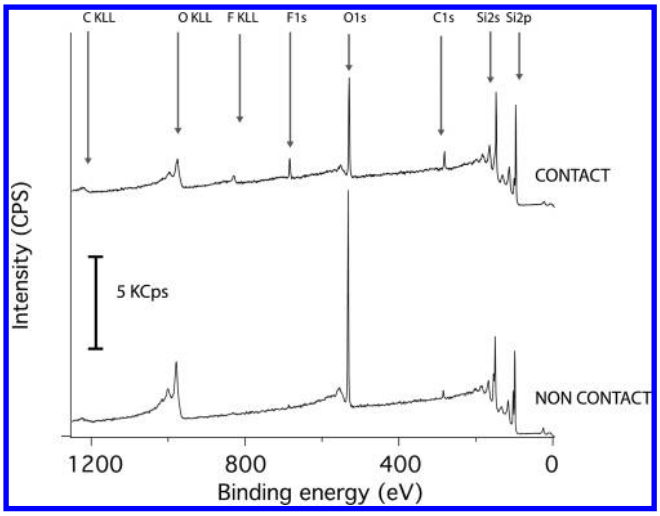

Figure 8. Survey XP-spectra of a silicon disk lubricated with [HMIM] FAP in the presence of humid air (45−55% RH): normal load, 4.5 N; sliding speed, 50 mm/min; Number of cycles, 200; radius, 3.2 mm.

Both spectra exhibit the presence of peaks characteristic of silicon oxide and silicon, (Si 2p, Si 2s, and O 1s). As in the case of the sample tribostressed inside the glovebox, the intensity of the O 1s signal is lower for the tribostressed area and fluorine is detected in both areas. On the other hand, the intensity of the F 1s signal is clearly lower with respect to the spectra acquired for samples tested in a nitrogen atmosphere. Additionally, the nitrogen signal is barely detectable either in the contact or in the noncontact areas, suggesting that no or a negligible amount of nitrogen-containing species is present in the tribolayer when moisture and oxygen are present during the test. The high-resolution spectra for this sample are reported in Figures 9 and 10.

The C 1s signal (Figure 9a) is similar to that observed for the sample tribostressed under a nitrogen atmosphere. The same curve-fitting model used in the previous case was applied: components representing the aliphatic carbon and carbon bonded to oxygen or nitrogen have been used for the noncontact area; an additional component on the low binding energy side was added for the contact area.

The chemical-state analysis of the F 1s signal (Figure 9b) is less straightforward compared to the case of the samples treated in nitrogen, as the signal-to-noise ratio is significantly lower for samples tribologically stressed in humid air. Nonetheless, the peak position is close to that observed for the tests carried out in nitrogen, suggesting a similar chemical environment. A significant broadening of the F 1s signal is observed for the spectra of the contact area. Using the same curve-fitting model adopted for the tests carried out under nitrogen and comparing the obtained results, the ratio of the intensities of the two components changed significantly. In the presence of humid air, inside the track, a decrease in the low-binding-energy component with respect to the high-binding-energy component is observed. Additionally, depending on the analyzed area, it was observed that the two-component model was not able to fit the F 1s perfectly on the higher-binding-energy side. This might be related to a contribution from debris that are present in larger amounts inside the wear track for tests carried out in the

dx.doi.org/10.1021/jp505998k | J. Phys. Chem. C 2014, 118, 29389−29400

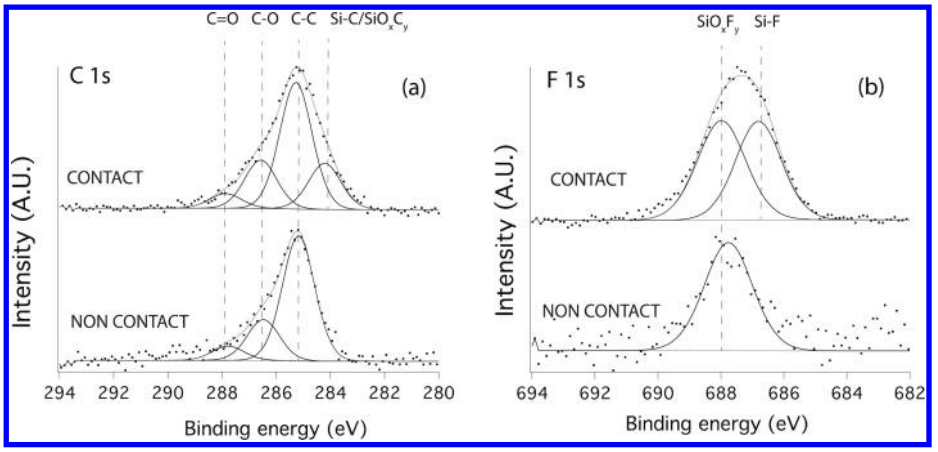

Figure 9. C 1s (a) and F 1s (b) regions of the XP-spectra of a silicon disk lubricated with [HMIM] FAP in the presence of humid air (45−55% RH): normal load, 4.5 N; sliding speed, 50 mm/min; number of cycles, 200; radius, 3.2 mm.

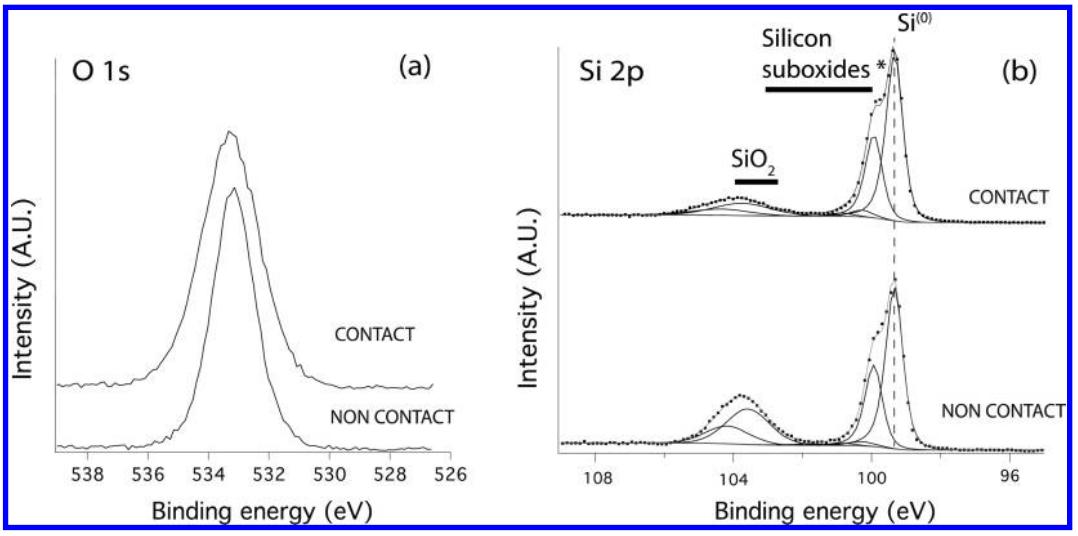

Figure 10. O 1s (a) and Si 2p (b) regions of the XP-spectra of a silicon disk lubricated with [HMIM] FAP in the presence of humid air (45−55% RH). Each Si signal is fitted with two components due to spin−orbit coupling ($2p_{3/2}$ and $2p_{1/2}$). The region labeled "Silicon suboxides" could also contain contributions from SiO_xF_y, SiC_xO_y, and SiN_xO_y: normal load, 4.5 N; sliding speed, 50 mm/min; number of cycles, 200; radius, 3.2 mm.

presence of humid air and might lead to a residual differential charging.

The oxygen 1s signal (Figure 10a) of the noncontact area (binding energy = 533.1 (0.1) eV, fwhm = 1.7 (0.1) eV) was similar to those obtained in the presence of a nitrogen atmosphere. The signal of the contact area was found to be broader, but no significant shift on the binding-energy scale was observed (binding energy = 533.1 (0.1) eV, fwhm = 2.0 (0.1) eV).

Similar behavior was observed for the Si 2p signal of the oxide, where no variation in the position of the SiO_2 component is observed (103.6 (0.2) eV), despite its decrease in intensity with respect to the noncontact area.

The spectra acquired on tribostressed samples in the presence of [EMIM] FAP showed the same features presented above for the [HMIM] FAP and are reported in the Supporting Information (Figures S6−8).

4. DISCUSSION

4.1. Effect of Environmental Conditions at Low Load. The evolution of the CoF during tribological testing carried out at 0.5 N and the related wear coefficient (Figure 1) were found to be highly affected by the environmental conditions for both investigated ILs. The contrast between the relatively smooth trend of friction with time and the negligible wear observed in the presence of a nitrogen atmosphere on the one hand, with the higher friction and measurable wear under humid conditions on the other, might suggest the existence of a thin lubricating film within the contact area, whose ability to separate the two surfaces is affected by the presence of water. As already mentioned, surface forces apparatus measurements carried out in our laboratory in the presence of humid air have shown that water molecules in the IL influences the structure of the films of [EMIM] FAP and [HMIM] FAP confined between atomically smooth mica surfaces and also the measured lateral force.[12] A significant increase in the time required to squeeze out layers was also measured with increasing confining pressure and this increase was more pronounced for the studied ILs under nitrogen than in humid air. These results suggested the enhancement of lubrication with confining pressure and the significant effect of water in degrading the lubrication. As an alternative, or in addition to, the existence of a thin lubricating film separating the two surfaces, adsorbed ions could be effective in preventing direct contact between asperities, as long

dx.doi.org/10.1021/jp505998k | J. Phys. Chem. C 2014, 118, 29389−29400

as the roughness of the sliding surfaces is limited to a few nanometers, that is, for the undamaged surfaces. In this case, the presence of water could disrupt the formation of a contiguous layer of adsorbed IL ions, negatively affecting the ability of the layer of ions to prevent the contact.

In order to rule out the possibility of hydrodynamic forces playing a role in these studies, an attempt was made to estimate the thickness of the lubricant film by using the Hamrock and Dowson model.[26] The viscosity of the two dried liquids is reported in Table 1. As their pressure-viscosity coefficients were not found in the literature, an approximate value of 17 GPa^{-1} is assumed for both ILs, which has been reported for the structurally similar 1-butyl-2,3-dimethylimidazolium FAP.[27] The mechanical parameters of the disk and the pin used for the calculation are reported in Table 2. Film thicknesses of 0.8 and 0.6 nm are predicted for dried [HMIM] FAP and [EMIM] FAP, respectively. Considering that the composite surface roughness for the used tribopair is ∼1.2 nm, a λ parameter (i.e., the ratio of the expected lubricant thickness and the composite surface roughness) less than 1 is obtained. This would suggest that, were the lubricant a simple oil, even the undamaged surfaces would be considered as operating in the boundary regime (i.e., the hydrodynamic forces are negligible), when applying a load of 0.5 N and at a sliding speed of 50 mm min^{-1}. The very fact that wear is below the detection limit in the absence of moisture suggests, however, that there is another protective mechanism (e.g., IL layering) at work. It should, however, be borne in mind that the Hamrock model might provide unreliable predictions in the case of film thicknesses of less than a few nanometers, and for very flat solid surfaces (i.e., having a R_q of the order of 1 nm).[28] In fact, deviations from the Hamrock prediction have been observed at low speeds for several ILs, leading to higher thickness values than those expected from EHL theory.[29]

Apart from modifying the structure of the confined lubricant, water may also contribute to the observed transition in the tribological behavior by increasing the rate of solvolysis of the siloxane bonds. Barnette et al.[18] investigated the friction and wear of vapor-lubricated silica-glass balls sliding against silicon wafers. No measurable wear and a constant friction were observed in the presence of *n*-pentanol vapor, while high wear and large fluctuations in friction were observed in the presence of humid argon. These findings were related to the rate of solvolysis of the siloxane bonds: that is, the exchange of Si-OH for Si-OR groups increasing the activation energy for the solvolysis of Si−O−Si bonds, leading to a lower wear rate in the presence of the alcohol. Since no evidence of chemisorption of the ions has been detected in the noncontact area, the mechanism proposed by Barnette et al. seems not to be applicable to our results. Nonetheless, the possibility that water could affect the rate of solvolysis of siloxane groups cannot be ruled out.

Our results show that in the case of [HMIM] FAP, an initial regime of low friction was observed (Figure S1). This finding might suggest that longer aliphatic chains of the adsorbed imidazolium cations might promote boundary-layer stability by means of stronger interchain dispersive interactions, also screening the surface from hydrolytic attack by water.

4.2. Effect of Environmental Conditions at High Load. The tests performed at an applied load of 4.5 N showed no low-wear regime under nitrogen.

For all tribological experiments, after an initial phase of the duration of around 20−50 turns, a steady state was reached, during which the CoF was found to be similar for both ILs and environmental conditions. In addition, upon switching from nitrogen to humid air, an increase in wear of the silicon disk and a larger amount of debris within the wear track were observed.

The differences in the amount of debris are likely related to the tribochemical processes taking place within the contact area. As demonstrated by the XPS results, the decomposition of the two ILs clearly takes place, leading to the formation of species that cannot be identified as adsorbed ions (see Table S3, Supporting Information). The decomposition of fluorinated ILs and reaction with the metal substrate has been reported for several tribopairs, including steel/aluminum[30] and steel/steel.[31] Most probably, the decomposition of the FAP anion leads to the formation of fluoride anions. The structurally similar exafluorophosphate anion (PF_6^-) is known to hydrolyze even in the absence of any mechanical stress, leading to the formation of hydrofluoric acid. Despite the higher stability of FAP anions, the conditions encountered during sliding can reasonably induce the cleavage of the P−F bond, either in the presence or absence of water, leading to the release of fluoride ions into the liquid.

In this work, two components having binding energies of 686.8 (0.1) and 687.9 (0.1) eV have been used for fitting the F 1s signals of the tribologically stressed samples. Haring et al.,[32] acquired the spectra of fluorinated silicon surfaces obtained after exposure of oxide-free silicon to XeF_2 and its conversion to oxyfluoride after exposure to water vapors. They reported a binding energy of 686.4 eV for the fluorinated silicon (Si−F) and a shift of +1.4−1.6 eV for the oxyfluorides. The differences from the data reported by Haring might derive from a different process being involved, leading to a different structure of the surface layer.

The F 1s peak measured outside the contact area (687.9 eV) indicates that fluoride not only reacts with the nascent silicon surface, but it can also be adsorbed on the silicon oxide layer outside the contact area. Inside the wear track the broadening and shift of this signal toward lower-binding-energy values (fitted by introducing the component centered at 686.8 eV) substantiate that part of the fluorine is directly bonded to the silicon surface.

The presence of water is expected to lead to the conversion of silicon fluorides to oxyfluoride inside the contact area and to an overall decrease of the amount of fluorine by hydrolysis, which is in agreement with results obtained for tests carried out in humid air (Figures 8−10).

The presence of humid air also affects the formation of nitrogen-containing species. A clearly detectable N 1s signal (398.2 (0.2) eV) was observed only inside the wear track of tribologically stressed samples in a nitrogen atmosphere. From a comparison with the literature data,[23] the signal could be ascribed to the presence of oxynitrides within the contact area. The presence of the small amount of dissolved water seems to be able to prevent the formation of this product or to induce its degradation, as in the case of silicon nitride, which is hydrolyzed as a consequence of sliding in the presence of humid air.[33]

With regard to the C 1s region, a shoulder toward lower binding energy was observed for both environmental conditions. As in the case of nitrogen, the peak could be related to the formation of silicon-containing species, such as silicon carbide or oxycarbide. The C 1s signal of pure silicon carbide has a binding energy of around 283.0 eV.[34] A higher

dx.doi.org/10.1021/jp505998k | J. Phys. Chem. C 2014, 118, 29389−29400

value (283.6 eV) has been reported in the case of silicon oxycarbide.[35] Alternatively, the existence of organic carbon bonded to silicon, as in the case of SAM of alkene on silicon, would lead to a signal having a binding energy of 283.9 eV.[36] In addition, it cannot be ruled out that graphitic carbon could also be present, as it would generate a signal among the aliphatic and carbidic components.[37]

Another effect related to the presence of humid air is the broadening of the SiO_x-related signals toward higher-binding-energy values, which could be related to the presence of silanol groups and adsorbed water. Compared to other metal oxides, in the case of SiO_2 the presence of −OH groups does not lead to large chemical shifts, but a broadening of both the Si 2p and O 1s signals has been reported for hydroxylated silica films on silicon substrates.[38] Nonetheless, a residual charging of the debris cannot be ruled out and might contribute to the observed broadening of the O 1s and Si 2p (SiO_x) signals.

In summary, the XPS analysis of the silicon wafers tribostressed in the presence of a nitrogen atmosphere indicates the formation of a complex mixture of silicon-based compounds, deriving from the mechanically induced reaction of silicon with the ions present within the contact area. For tests carried out in humid air, an overall decrease in the signal intensity related to these species is observed, while the formation of silanol groups seems to take place. On the basis of these observations, we propose that the presence of water and oxygen induce the hydrolysis and oxidation of the species formed at the silicon surface, leading to an increase in the wear of silicon and greater formation of debris.

It is worth noting that the presence of water and oxygen seems to mainly affect tribochemical reactions involving the nascent silicon surface, as wear of the fused-silica-glass pins was found to be marginally affected or not affected at all by the environmental conditions. In addition, the large standard deviation associated with the data does not allow obtaining a conclusive indication of the role of the environmental conditions on the wear of the pins.

Comparing the results obtained with the [HMIM] FAP and [EMIM] FAP, no relevant effects were observed in terms of friction (during the steady state), wear, or chemical composition of the tribostressed surfaces. These findings suggest that, under the experimental conditions presented here, the difference in length of the aliphatic chain attached to the imidazolium ion plays a minor role in affecting the mechanism of lubrication of the two ILs.

On the other hand, it is evident that significant differences between tests carried out with [HMIM] FAP and [EMIM] FAP were observed during the initial turns. The environmental conditions were also found to affect the initial trend of friction (Figures S2−5, Supporting Information). These findings suggest that, as long as the damage of the surfaces is limited, the thin film of IL is initially able to prevent asperity-asperity contact. Progressively, damage of the surface takes place, eventually leading to a regime dominated by contact between sliding surfaces and chemical changes taking place within the tribologically stressed area. Comparing the trends of friction observed during the initial turns, it is observed that for tests carried out under nitrogen, an increase of friction with time is observed, especially in the case of [HMIM] FAP. In contrast, in the presence of humid air CoF was high during the first few turns, particularly in the case of tests carried out with [EMIM] FAP. These results might indicate that the ability of the IL film to prevent damage of silica surfaces is negatively affected by the presence of water in the contact area. Additionally, [HMIM] FAP seems to be better than [EMIM] FAP in preventing wear during the initial regime, in agreement with the results obtained at low load.

4.3. Comparison of Friction and Wear at High and Low Load. Friction and wear coefficients appear to depend strongly on load (Figures 1c and 2c): in the presence of humid air (i.e., when the confined IL layer is ineffective in preventing contact between asperities), higher friction and wear coefficients of the silicon disks were measured at the lower load. On the other hand, the wear coefficient of the fused silica pins was found to be unaffected by the applied load.

First, it has to be considered that tests carried out at different loads differ in terms of apparent contact area, resulting in average applied pressures that are not proportional to the applied loads. This may play a role in the differences in measured wear of the disks.

The experimental results indicate that since structure and composition of the tribostressed areas are different at the different loads, the wear mechanism may be different. In particular, the wear products formed at higher load (4.5 N) appear to exhibit better lubrication than those formed in low-load tests (0.5 N).

It should be noted that, despite silicon being harder than fused silica, the wear of the pins was always found to be lower than that of the disks. These findings support the idea that, under the selected experimental conditions, the wear is not entirely governed by an abrasive mechanism but also by the synergic contribution from oxidation and tribochemical reactions taking place within the contact area. These seem to mainly affect the (nascent) elemental silicon surface. This might explain, on the one hand, the higher wear coefficients measured for the disks, and, on the other, the negligible influence of applied load and environmental conditions on the wear of the fused silica pins.

5. CONCLUSIONS

The tribological behavior of silica/silicon tribopairs lubricated with FAP-based ILs has been investigated at room temperature under two different environmental conditions, namely, pure nitrogen and humid air (45−55% RH). Environmental conditions were found to affect the mechanism of lubrication in different ways, depending on the applied load.

In the presence of a nitrogen atmosphere, a smooth trend of friction and absence of measurable wear were observed under a load of 0.5 N, indicating that the IL layer is able to prevent contact between asperities. The large increases in friction and wear observed when switching to humid air indicate that water modifies the structure of the confined lubricant, degrading its lubrication properties. The hydrolysis of siloxane bonds under mechanical stress might also contribute to the observed large increase of wear in humid air.

At higher load (4.5 N), after the initial few turns, a steady-state condition is reached: very similar CoF values were observed for the different ILs and environmental conditions, suggesting that asperity contact and tribochemical reactions dominate this tribological regime.

The wear coefficient of the fused silica pins was found to be lower than that of the harder silicon disks, suggesting that the wear mechanism is affected by the different reactivities of the two tribostressed materials. The dependence of the wear rate of the silicon disks by environment and load also suggest that the

tribochemical processes taking place within the contact area are mainly affecting the silicon in its nascent state.

The XPS analysis showed that the intensity of the signals related to fluorine-containing (Si−F, SiF_yO_x) and nitrogen-containing (SiN_xO_y) species is significantly lower for tests carried out in the presence of humid air. This result indicates that the hydrolysis or oxidation of these silicon-containing species, deriving from the mechanically induced reaction of the nascent silicon surface with ions, is related to the increase of wear of the silicon wafer in the presence of humid air. The larger amount of debris formed in the presence of humid air and the indication of hydrated forms of SiO_x from the XPS analysis support this hypothesis.

■ ASSOCIATED CONTENT

Supporting Information

The peak-fitting parameters for the high-resolution XP-spectra of tribostressed samples are reported in Tables S1 and S2. A list of the binding energies used of the compounds considered for the chemical-state analysis of the tribostressed wafers is reported in Table S3. Three replicas of a tribological test carried out in the presence of humid air with [HMIM] FAP as a lubricant, applying a load of 0.5 N, are reported in Figure S1. Replicas of the tribological tests carried out applying a load of 4.5 N are reported in Figures S2−5. The survey and high-resolution spectra of tribostressed silicon disks lubricated with [EMIM] FAP, applying a load of 4.5 N, are reported in Figures S6−8. Optical and scanning electron micrographs of tribostressed disks lubricated with [EMIM] FAP are reported in Figures S9 and S10. This material is available free of charge via the Internet at http://pubs.acs.org.

■ AUTHOR INFORMATION

Corresponding Author

*Phone: +41-44-632-5850. Fax: +41-44-633-1027. E-mail: nspencer@ethz.ch.

Notes

The authors declare no competing financial interest.

■ ACKNOWLEDGMENTS

The authors wish to express their gratitude to Mr. Clément Cremmel for his support in the acquisition of the SEM picture of the tribostressed silicon disks. The ETH Zurich Laboratory for Microelemental Analysis is thanked for their measurements of water uptake in the ILs. We are most grateful to the Swiss National Science Foundation for their funding of this research through their *Sinergia* program.

■ REFERENCES

(1) Wilkes, J. S.; Zaworotko, M. J. Air and Water Stable 1-Ethyl-3-methylimidazolium Based Ionic Liquids. *J. Chem. Soc., Chem. Commun.* **1992**, 965−967.

(2) Gordon, C. M.; Muldoon, M. J.; Wagner, M.; Hilgers, C.; Davis, J. H.; Wasserscheid, P., Synthesis and Purification. *Ionic Liquids in Synthesis*; Wiley-VCH Verlag GmbH & Co. KGaA: New York, 2008; pp 7−55.

(3) Plechkova, N. V.; Seddon, K. R. Applications of Ionic Liquids in the Chemical Industry. *Chem. Soc. Rev.* **2008**, *37*, 123−150.

(4) Armand, M.; Endres, F.; MacFarlane, D. R.; Ohno, H.; Scrosati, B. Ionic-Liquid Materials for the Electrochemical Challenges of the Future. *Nat. Mater.* **2009**, *8*, 621−629.

(5) Weingärtner, H. Understanding Ionic Liquids at the Molecular Level: Facts, Problems, and Controversies. *Angew. Chem., Int. Ed.* **2008**, *47*, 654−670.

(6) Palacio, M.; Bhushan, B. A Review of Ionic Liquids for Green Molecular Lubrication in Nanotechnology. *Tribol. Lett.* **2010**, *40*, 247−268.

(7) Bermúdez, M.-D.; Jiménez, A.-E.; Sanes, J.; Carrión, F.-J. Ionic Liquids as Advanced Lubricant Fluids. *Molecules* **2009**, *14*, 2888−2908.

(8) Pisarova, L.; Gabler, C.; Dörr, N.; Pittenauer, E.; Allmaier, G. Thermo-oxidative Stability and Corrosion Properties of Ammonium Based Ionic Liquids. *Tribol. Int.* **2012**, *46*, 73−83.

(9) Horn, R. G.; Evans, D. F.; Ninham, B. W. Double-Layer and Solvation Forces Measured in a Molten-Salt and Its Mixtures with Water. *J. Phys. Chem.* **1988**, *92*, 3531−3537.

(10) Perkin, S. Ionic Liquids in Confined Geometries. *Phys. Chem. Chem. Phys.* **2012**, *14*, 5052−5062.

(11) Li, H.; Rutland, M. W.; Atkin, R. Ionic Liquid Lubrication: Influence of Ion Structure, Surface Potential and Sliding Velocity. *Phys. Chem. Chem. Phys.* **2013**, *15*, 14616−14623.

(12) Espinosa-Marzal, R. M.; Arcifa, A.; Rossi, A.; Spencer, N. D. Microslips to "Avalanches" in Confined, Molecular Layers of Ionic Liquids. *J. Phys. Chem. Lett.* **2013**, *5*, 179−184.

(13) Espinosa-Marzal, R. M.; Arcifa, A.; Rossi, A.; Spencer, N. D. Ionic Liquids Confined in Hydrophilic Nanocontacts: Structure and Lubricity in the Presence of Water. *J. Phys. Chem. C* **2014**, *118*, 6491−6503.

(14) Ueno, K.; Kasuya, M.; Watanabe, M.; Mizukami, M.; Kurihara, K. Resonance Shear Measurement of Nanoconfined Ionic Liquids. *Phys. Chem. Chem. Phys.* **2010**, *12*, 4066−4071.

(15) Kondo, Y.; Yagi, S.; Koyama, T.; Tsuboi, R.; Sasaki, S. Lubricity and Corrosiveness of Ionic Liquids for Steel-on-Steel Sliding Contacts. *Proc. Inst. Mech. Eng., Part J* **2012**, *226*, 991−1006.

(16) Nainaparampil, J. J.; Eapen, K. C.; Sanders, J. H.; Voevodin, A. A. Ionic-Liquid Lubrication of Sliding MEMS Contacts: Comparison of AFM Liquid Cell and Device-Level Tests. *J. Microelectromech. Syst.* **2007**, *16*, 836−843.

(17) Komvopoulos, K. Surface Engineering and Microtribology for Microelectromechanical Systems. *Wear* **1996**, *200*, 305−327.

(18) Barnette, A. L.; Asay, D. B.; Kim, D.; Guyer, B. D.; Lim, H.; Janik, M. J.; Kim, S. H. Experimental and Density Functional Theory Study of the Tribochemical Wear Behavior of SiO_2 in Humid and Alcohol Vapor Environments. *Langmuir* **2009**, *25*, 13052−13061.

(19) Hopcroft, M. A.; Nix, W. D.; Kenny, T. W. What is the Young's Modulus of Silicon? *J. Microelectromech. Syst.* **2010**, *19*, 229−238.

(20) Giardini, A. Study of the Directional Hardness in Silicon. *Am. Mineral.* **1958**, *43*, 957−969.

(21) Keister, J. W.; Rowe, J. E.; Kolodziej, J. J.; Niimi, H.; Tao, H.-S.; Madey, T. E.; Lucovsky, G. Structure of Ultrathin SiO_2/Si(111) Interfaces Studied by Photoelectron Spectroscopy. *J. Vac. Sci. Technol., A* **1999**, *17*, 1250−1257.

(22) Beamson, G.; Briggs, D. *High Resolution XPS of Organic Polymers: The Scienta ESCA300 Database*; John Wiley & Sons: Chichester, U.K., 1992.

(23) Cerofolini, G. F.; Caricato, A. P.; Meda, L.; Re, N.; Sgamellotti, A. Quantum-Mechanical Study of Nitrogen Bonding Configurations at the Nitrided SiO_2 Interface via Model Molecules. *Phys. Rev. B* **2000**, *61*, 14157−14166.

(24) Seah, M. P.; Spencer, S. J. Ultrathin SiO_2 on Si IV. Intensity Measurement in XPS and Deduced Thickness Linearity. *Surf. Interface Anal.* **2003**, *35*, 515−524.

(25) McFeely, F. R.; Morar, J. F.; Shinn, N. D.; Landgren, G.; Himpsel, F. J. Synchrotron Photoemission Investigation of the Initial Stages of Fluorine Attack on Si Surfaces: Relative Abundance of Fluorosilyl Species. *Phys. Rev. B* **1984**, *30*, 764−770.

(26) Stachowiak, G. W.; Batchelor, A. W. Elastohydrodynamic Lubrication. In *Engineering Tribology*, 3rd ed.; Stachowiak, G. W., Batchelor, A. W., Eds.; Butterworth-Heinemann: Burlington, 2006; pp 335−424.

(27) Fernández, J.; Paredes, X.; Gaciño, F. M.; Comuñas, M. J. P.; Pensado, A. S. Pressure-Viscosity Behaviour and Film Thickness in Elastohydrodynamic Regime of Lubrication of Ionic Liquids and Other Base Oils. *Lubr. Sci.* **2013**, 1−14.

(28) Spikes, H. A. Direct Observation of Boundary Layers. *Langmuir* **1996**, *12*, 4567−4573.
(29) Xiao, H.; Guo, D.; Liu, S.; Pan, G.; Lu, X. Film Thickness of Ionic Liquids under High Contact Pressures as a Function of Alkyl Chain Length. *Tribol. Lett.* **2011**, *41*, 471−477.
(30) Somers, A. E.; Biddulph, S. M.; Howlett, P. C.; Sun, J.; MacFarlane, D. R.; Forsyth, M. A Comparison of Phosphorus and Fluorine Containing IL Lubricants for Steel on Aluminium. *Phys. Chem. Chem. Phys.* **2012**, *14*, 8224−8231.
(31) Minami, I.; Kita, M.; Kubo, T.; Nanao, H.; Mori, S. The Tribological Properties of Ionic Liquids Composed of Trifluorotris-(pentafluoroethyl) Phosphate as a Hydrophobic Anion. *Tribol. Lett.* **2008**, *30*, 215−223.
(32) Haring, R. A.; Liehr, M. Reactivity of a Fluorine Passivated Silicon Surface. *J. Vac. Sci. Technol., A* **1992**, *10*, 802−805.
(33) Fischer, T. E.; Tomizawa, H. Interaction of Tribochemistry and Microfracture in the Friction and Wear of Silicon Nitride. *Wear* **1985**, *105*, 29−45.
(34) Kusunoki, I.; Igari, Y. XPS Study of a SiC Film Produced on Si(100) by Reaction with a CH_2H_2 Beam. *Appl. Surf. Sci.* **1992**, *59*, 95−104.
(35) Guinel, M. J.-F.; Norton, M. G. Oxidation of Silicon Carbide and the Formation of Silica Polymorphs. *J. Mater. Res.* **2006**, *21*, 2550−2563.
(36) Nemanick, E. J.; Hurley, P. T.; Webb, L. J.; Knapp, D. W.; Michalak, D. J.; Brunschwig, B. S.; Lewis, N. S. Chemical and Electrical Passivation of Single-Crystal Silicon(100) Surfaces through a Two-Step Chlorination/Alkylation Process. *J. Phys. Chem. B* **2006**, *110*, 14770−14778.
(37) Díaz, J.; Paolicelli, G.; Ferrer, S.; Comin, F. Separation of the sp3 and sp2 Components in the C1s Photoemission Spectra of Amorphous Carbon Films. *Phys. Rev. B* **1996**, *54*, 8064−8069.
(38) Miller, M. L.; Linton, R. W. X-ray Photoelectron Spectroscopy of Thermally Treated Silica (SiO_2) Surfaces. *Anal. Chem.* **1985**, *57*, 2314−2319.